

# FUSION OF HYPERSPECTRAL IMAGES AND HEIGHT MODELS USING EDGE PROBABILITY

*J. Avbelj* \*

Technische Universität München \*  
Chair of Remote Sensing Technology  
Arcisstr. 21, 80333 Munich, Germany

*R. Müller, P. Reinartz*

German Aerospace Center \*  
Earth Observation Center  
Oberpfaffenhofen, 82234 Wessling, Germany

## ABSTRACT

We propose a method for data fusion of hyperspectral images (HSI) and digital surface models (DSM) basing on the edge probabilities from both datasets. A height discontinuity in DEM and change in material in HSI represent the high probability of an edge. Edge probabilities are computed in scale-space and combined according to the Gaussian mixture model. The reliability of the datasets can be included into this model as a prior knowledge. The method is tested on an urban area, where building boundaries represent the high probabilities of an edge in both datasets. Our results show, that the probabilistic fusion technique is advantageous where boundary detected from only one dataset are unreliable.

**Index Terms**— Hyperspectral, Fusion, Digital Elevation Model, Image Processing

## 1. INTRODUCTION

Usage of different datasets enable to extract better knowledge about objects of interest in a scene. The HSI contain information about spectral properties of the objects, i.e. every pixel from HSI is characterized by the spectral signature. Thus, the HSI enable to identify the materials of the pixels in the observed area. DSM include additional information about the surface compared to the HSI, they comprise heights of ground and aboveground objects. Consequently, different information included in HSI and DSM is advantageous for the data fusion. However, finding mutual features to combine two so diverse datasets is a challenging task. Boundaries of some object, such as building boundaries or forest edge, appear as a material change in mixed pixel in HSI, and as a height change in DSM. This boundaries can be detected as image edges and used for the data fusion. Computing the probability of an edge evades the hard decision if a pixel belongs to an edge or not, and the fused representation is also probabilistic. In this contribution, we denote the importance of scale-space representation for edge detection in Section 2, and propose a method for image fusion of HSI and DSM in Section 3 basing on the edge probabilities.

## 2. PROBABILITY OF AN EDGE

In this Section, the motivation for using scale-space for edge detection is given, after edge detection in images and scale-space are defined.

### 2.1. Edge Detection

An edge in an image is an abrupt change of intensity and represents a boundary between two regions. Image  $I$  is a sampled representation of a continuous 2D function  $f(x, y)$ , where  $x, y$  variables. In this section, the edge detection principles are first explained on 1D signals, and afterwards extended to 2D signals, on an example of an ideal step edge.

A continuous 1D signal is given by a function  $f(x)$ . Many classical edge detection algorithms such as Canny edge detector [1] base on smoothing the image with the Gaussian filter, and then compute a magnitude of the first derivative of a signal  $|f'(x)| = |f_x|$ . In a stationary point, that is local minimum, maximum or inflection point,  $f_x = 0$ , elsewhere the first derivative is larger for the larger changes in intensity. Measured signals are a discrete representation of continuous signals, so the first derivative can be approximated by the discrete derivative  $f_x = f(x) - f(x - 1)$ , or central discrete derivative  $f_x = f(x - 1) - f(x + 1)$ . The edge can also be detected by finding zero crossings of a second derivative of a signal  $f_{xx}$ . [2] suggest to detect edges using two conditions. First, the edge exists, if  $f_{xx}$  has a zero crossing, and

$$\left| \frac{f_{xx}}{f_{xxx}} \right| < \Delta x \quad (1)$$

where  $\Delta x$  is half of a pixel. Some of detected zero crossings correspond to the phantom edges. A second condition must be fulfilled [3] to avoid phantom edges

$$f_x f_{xxx} < 0. \quad (2)$$

The edge detection using derivatives can be extended from 1D to 2D signals by convolving the image, i.e. 2D signal, with the derivative filter in two perpendicular directions  $x, y$ . A

derivative in an edge direction is computed by a linear combination of basis filters, and the edge direction is given by  $\phi = \text{atan}\sqrt{f_x^2/f_y^2}$ .

## 2.2. Scale-Space Representation

Edges in natural images or earth observation images are not ideal, as assumed in the previous Subsection 2.1. For example, profile of a building is taken from DSM and a task is to detect an edge of a building. The building profile is a 1D discrete signal, thus an edge can be detected using discrete derivative. The result depends on a selected step size of a discrete derivative. Only some step sizes of a discrete derivative return meaningful results; too large or too small step size results in failing to detect the edge or detecting noise, respectively. A scale-space representation of the signals is a methodology that can handle the concept of different scales [4]. A continuous signal of an arbitrary dimension  $f$  belongs to a scale-space family  $L$  of a signal, given by convolution of the signal with Gaussian kernel  $g$ . A scale-space representation of a 2D signal  $f(x, y)$  is

$$L(x, y; t) = g(x, y; t) * f(x, y) \quad (3)$$

where  $t$  is a scale parameter, and  $g$  is a 2D Gaussian kernel with variance  $t$

$$g(x, y; t) = \frac{1}{2\pi t} e^{-(x^2+y^2)/2t}. \quad (4)$$

Scale-space representation at zero scale  $t = 0$  is equal to the original signal

$$f = L(x, y; t = 0). \quad (5)$$

Physical interpretation of a scale-space family is the *diffusion equation*

$$\partial_t L = \frac{1}{2} \nabla^2 L = \frac{1}{2} \partial_{xx} L \quad (6)$$

with the initial condition given by Eq. 5. An intensity of a pixel in an image can be interpreted as a temperature, and  $f(x, y)$  as heat distribution at time  $t = 0$ . A solution of the diffusion equation is a scale-space representation of a signal  $f$ , e.g. a heat distribution  $f$  over time  $t$  in an infinite homogeneous medium [4].

## 2.3. Edges in Scale-Space

Convolving a discrete signal  $f$  with the sampled Gaussian leads in some cases to faulty second derivatives as shown in [4], so they suggest to convolve the signal with the discrete Gaussian kernel  $T$

$$\begin{aligned} L(x; t) &= \sum_{n=-\infty}^{\infty} T(n; t) f(x - n) = \\ &= \sum_{n=-\infty}^{\infty} e^{-t} I_n(t) f(x - n) \end{aligned} \quad (7)$$

where  $I_n$  is a modified Bessel function of integer order  $n$ . Discrete Gaussian kernel is a scale-space kernel, because it retains the scale-space properties of a signal convolved with it between an arbitrary level of scale  $t$ .

## 3. FUSION OF HSI AND DSM

In this section we propose a methodology how to fuse the HSI and DSM using the probabilities of edges from both datasets. The probability of an edge is high on the building boundaries in DSM and HSI, representing height discontinuity and change of material, respectively. The approximate position of the building boundary must be known to define roofing material, then the probabilities of the boundaries can be used to combine the datasets. The precondition for suggested method is pixel-precise registration of the used datasets.

### 3.1. Roofing Material Selection

The roofing materials largely differ in the spectral properties and are not unique, e.g. concrete can be used for roofing material as well as for pavement. Thus, we suggest to automatically extract the spectral signatures of roofing materials locally, using height information from DSM and HSI. The DSM in normalized (nDSM) and local peaks in nDSM corresponding to the building roofs or the high vegetation are selected. The seed points belonging to the high vegetation are removed by calculating Normalized Difference Vegetation Index from HSI. Then, local peaks are connected according to the 4-pixel neighbourhood and outliers in each region are discarded with regard to spectral properties of each pixel. From the remaining seed points, the reference spectrum is defined for each region. In [5] the procedure of selecting spectrum of roofing materials and seed points is explained in detail.

### 3.2. Edge Probabilities

[2] proposed a probabilistic framework for edge detection in natural images, defining probability of an edge for every pixel. They model the edges according to Eq. 1 and Eq. 2 assuming Gaussian noise  $\sigma_n$ , realize the image derivatives and define their statistical properties in scale-space. We apply this methodology directly to calculate the edge probabilities in nDSM.

We assume linear mixture model with full additivity constrain, i.e. abundances of each pixel sum up to one and are non-negative on an interval  $[0, 1]$ . Our aim is to compute the probability of an edge, which is indicated by a change of roofing material in HSI on the building boundary. Both, abundances and probabilities are bounded on the interval  $[0, 1]$  therefore, the abundance maps for roofing materials are needed to estimate the edge probability. A complete spectral library was not available for the given dataset, so the material

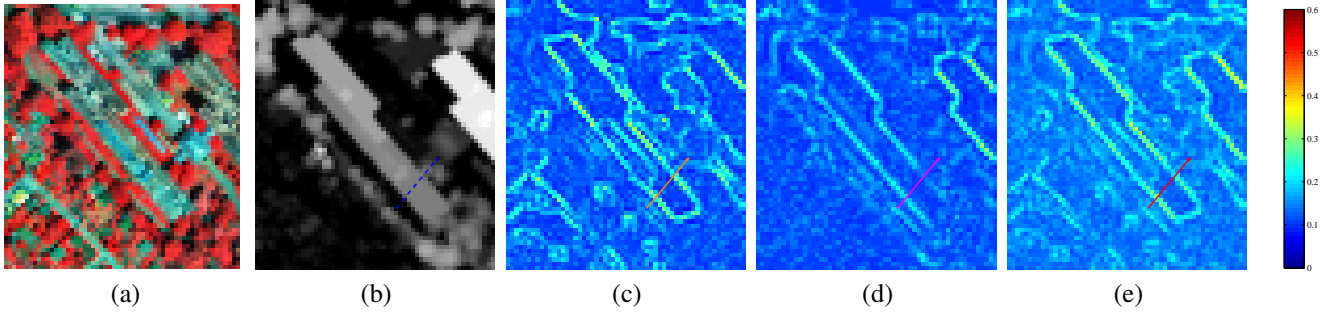


**Fig. 1.** Fusion of HSI and DSM with edge probabilities on an example of one building. Input HSI in false colour composite (a) and DSM (b). Edge probabilities of the roofing material from the building (c), and edge probabilities of the DSM (d). Combined edge probabilities (e). The colour bar for all the probability maps is the same (c,d,e). The lines on b-e present location of profiles in Fig. 4.

map is defined as similarity between roofing material and every pixel in HSI. We suggest to use Spectra Angle Distance (SAD) as similarity measure, because it is insensitive to the illumination. Then, the edge probability of a material is calculated from the material maps using the same framework as for probabilities in nDSM.

### 3.3. Fusion of Edge Probabilities

The probability of an edge is separately estimated from two independent datasets, DSM and HSI. If both datasets, i.e. components, are normal distributed  $\sim \mathcal{N}(\mu_k, \Sigma_k)$  with  $\mu_k$  mean and  $\Sigma_k$  covariance, they can be combined according to the Gaussian Mixture Model [6]. The probability of an edge is given by marginal density

$$p(\text{edge}) = \sum_{k=1}^2 \pi_k \mathcal{N}(x|\mu_k, \Sigma_k) = \sum_{k=1}^2 p(k)p(\text{edge}|k) \quad (8)$$

where  $p(\text{edge}|k)$  is probability of edge given component  $k$ , and  $\pi_k$  are mixing coefficients equal to prior probability  $p(k)$  of picking  $k^{\text{th}}$  component. Mixing coefficients are non negative  $0 \leq \pi_k \leq 1$  and they sum up to one  $\sum_{k=1}^2 \pi_k = 1$ .

## 4. EXPERIMENT

### 4.1. Data Description

Two datasets of a residential area of the city of Munich are used for fusion, HSI and DEM, both acquired in June 2012. First dataset, HSI was acquired with a HySpex hyperspectral camera (Fig. 2, left). The system consists of two sensors, VNIR and SWIR camera, providing two images that are combined in post processing. For the tests we used the VNIR image only, consisting of 160 channels in a spectral range of 410-990 nm, and 3.7 nm sampling interval. Four channels were removed before processing due to the high noise level.

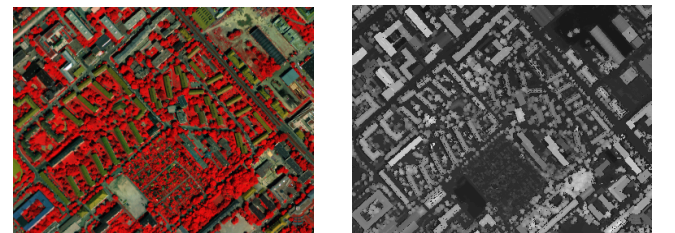


**Fig. 2.** Input data sets: HSI as false colour composite (left) and DSM (right), both with spatial resolution of 2 m.

Second dataset, DSM was computed from multi-view optical images using semi global matching (Fig. 2, right). The optical images were acquired with the 3K camera system, consisting of three non-metric cameras, one looking at nadir and two looking oblique sideways [7]. A lidar DSM with the average density of 1.69 points/m<sup>2</sup> is resampled with the nearest neighbour method to 1 m grid and used to compare computed edge probabilities and building profile.

### 4.2. Results

The DSM and HSI are smoothed with the discrete Gaussian kernel of size 3x3 pixels and  $t = 1$ , then the edge probabilities are computed with selected noise level  $\sigma_n = 1$ . The results are presented on an example of one building (Fig. 1, Fig. 4) and for complete area for one roofing material (Fig. 3). We assume no prior information, so the mixing coefficient are  $\pi_1 = \pi_2 = 0.5$ .

Edge probabilities for a building in Fig. 1a (HSI) and Fig. 1b (DEM) are computed and combined (Fig. 1e). Next to a part of a northeast and southeast side of a building are high trees, so the edge probability computed from DSM (Fig. 1d) is low, compared to the edge probability computed from HSI (Fig. 1c). This can also be observed in a profile (Fig. 4), between 10<sup>th</sup> and 11<sup>th</sup> pixel (pix), where edge probability

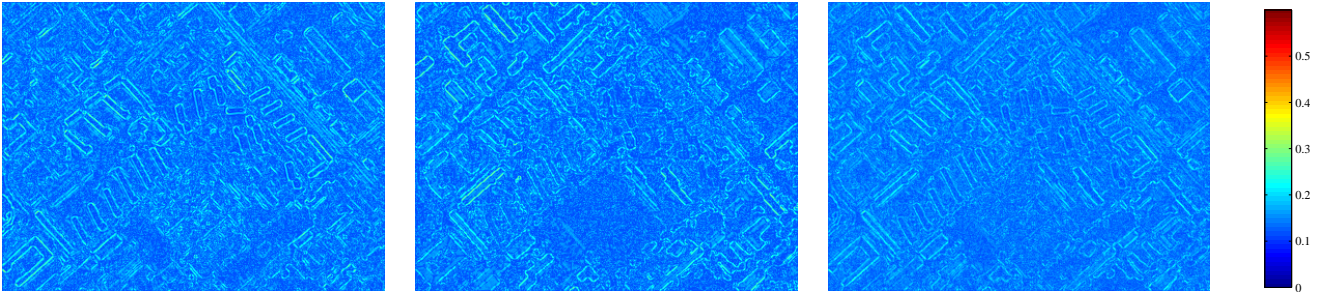


**Fig. 3.** Fusion of HSI and DSM with edge probabilities on an example of red roofing tiles material. Edge probabilities for one material - red roofing tiles (left), edge probabilities of the DSM (centre) and combined edge probabilities (right).

computed from HSI is high (orange line), but low computed from DSM (magenta line). In this case, the combination of edge probabilities is advantageous (Fig. 4, red line). What is more, in a case where both probabilities are high, e.g. in Fig. 4, around  $2.5^{th}$  pix, the fusion has no significant influence.

The first peak detected with a fusion technique has a shift of 0.6 pixel (pix) compared to the peak in the lidar DSM (Fig. 4). We assume this shift is a consequence of not precise coregistration between 3K and lidar DSM and their positional accuracy. The second peak is good localized in the fusion result, it coincides with the peak in the lidar DSM.

## 5. CONCLUSIONS AND FUTURE WORK

We presented a probabilistic approach for data fusion of HSI and DSM using detected edges in scale-space. Our experiment shows, that probability of edges in fused result is higher compared to the probabilities from a single image input. The usage of HSI instead of multispectral images is of a crucial importance for the proposed method, because HSI enable to define material maps. We used SAD similarity measure, however any other similarity measure or unmixing results can be used. Further experiments for different target objects should be performed and quality of the fusion estimated to fully evaluate the proposed method. In addition, the fused result has well-defined edges and can support classification techniques in the border areas of two classes. In this contribution, we assumed that the datasets are registered, but the edge probability maps have a potential to be used for precise coregistration of multi-modal datasets.

## 6. REFERENCES

[1] J. Canny, "A computational approach to edge detection," *IEEE Transactions on Pattern Analysis and Machine Intelligence*, vol. PAMI-8, no. 6, pp. 679–698, November 1986.

[2] D.H. Marimont and Y. Rubner, "A probabilistic framework for edge detection and scale selection," in *Sixth*

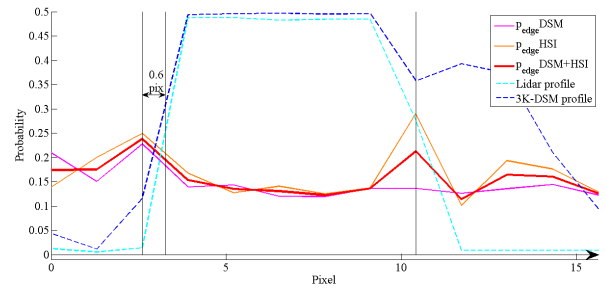


**Fig. 4.** Profile of fused edge probabilities from HSI and DSM on an example of one building. Full lines represent the edge probability computed from DSM (magenta), HSI (orange) and combined edge probability (red). Dashed lines are scaled profiles of the lidar (cyan) and 3K DSM (blue), respectively. The black vertical lines denote the position of edges.

*International Conference on Computer Vision*, January 1998, pp. 207–214.

[3] J.J. Clark, "Authenticating edges produced by zero-crossing algorithms," *IEEE Trans. Pattern Anal. Mach. Intell.*, vol. 11, no. 1, pp. 43–57, 1989.

[4] T. Lindeberg, *Scale-space theory in computer vision*, Kluwer Academic, Boston, 1994.

[5] J. Avbelj, "Spectral information retrieval for sub-pixel building edge detection," *ISPRS Annals of Photogrammetry, Remote Sensing and Spatial Information Sciences*, vol. I-7, pp. 61–66, July 2012.

[6] C.M. Bishop, *Pattern Recognition and Machine Learning*, Springer, February 2007.

[7] F. Kurz, S. Türmer, O. Meynberg, D. Rosenbaum, H. Runge, P. Reinartz, and J. Leitloff, "Low-cost optical camera systems for real-time mapping applications," *PFG Photogrammetrie, Fernerkundung, Geoinformation*, vol. 2012, no. 2, pp. 159–176, May 2012.